



Well-designed polyphenylene PEMs with high proton conductivity and chemical and mechanical durability for fuel cells

Journal:	<i>Journal of Materials Chemistry A</i>
Manuscript ID	TA-ART-12-2021-010480.R1
Article Type:	Paper
Date Submitted by the Author:	30-Jan-2022
Complete List of Authors:	Liu, Fanghua; University of Yamanashi, Clean Energy Research Miyatake, Kenji; University of Yamanashi, Clean Energy Research

ARTICLE

Well-designed polyphenylene PEMs with high proton conductivity and chemical and mechanical durability for fuel cells

Fanghua Liu^a and Kenji Miyatake^{*,b,c,d}Received 00th January 20xx,
Accepted 00th January 20xx

DOI: 10.1039/x0xx00000x

For highly proton conductive and durable proton exchange membranes, we designed and synthesized a new series of sulfonated polyphenylene ionomers (SPP-TFP) containing trifluoromethyl substituents with different ion exchange capacity (IEC). The resulting ionomers had high molecular weight ($M_n = 51.2\text{--}123.4$ kDa and $M_w = 96.1\text{--}556.1$ kDa) with reasonable polydispersity (3.8–5.4). The ionomers were highly soluble in some organic solvents such as DMSO and ethanol and provided bendable and ductile membranes by solution casting. SPP-TFP-3.5 membrane exhibited the best balanced properties as proton exchange membranes; the proton conductivity was 7.5 mS cm^{-1} at 20% RH and 80 °C and the maximum strain was $155 \pm 5\%$. The fuel cell performance of the SPP-TFP-3.5 membrane was comparable with that of Nafion NRE 211 membrane. Furthermore, in the accelerated combined chemical and mechanical durability test based on wet/dry cycling at open circuit voltage (OCV) at 90 °C supplying H_2 (anode) and air (cathode), the SPP-TFP-3.5 membrane (9847 cycles and 46.5 h) outperformed Nafion NRE 211 (8788 cycles and 41.5 h). Furthermore, compared with Nafion NRE 211 ($46.7\text{ }\mu\text{V h}^{-1}$ of the average decay), SPP-TFP-3.5 showed negligible change in the cell voltage at 0.15 A cm^{-2} under 90 °C and 30% RH (air/ H_2) for 300 h. Such high durability and performance in practical fuel cells have not been reported for aromatic ionomer membranes.

Introduction

Proton conducting membranes or proton exchange membranes (PEMs) are one of the essential components in electrochemical devices, such as fuel cells, electrochemical sensors, displays, and water electrolyzers.^{1–3} In the past decades, owing to high proton conductivity, mechanical properties and *ex-situ* chemical stability (in Fenton's reagent), perfluorosulfonic acid (PFSA) membranes such as Nafion produced by Dupont have been commercially available, state-of-the-art benchmark PEMs for fuel cell applications.^{4–6} However, inherent shortcomings of perfluorinated polymer structure involve restricted molecular design, complicated synthesis, low glass transition temperature (T_g), and high gas permeability, all of which may limit high temperature operable, durable, and low-cost fuel cells required for wide-spread dissemination, in particular, in automobile applications.^{7–11}

Recently, polyphenylene (PP) based ionomers have attracted as alternative PEMs, that could potentially overcome those issues associated with PFSA-PEMs.^{12–16} Compared to a number of other aromatic polymer-based PEMs such as sulfonated poly(arylene ether)s,^{17–19} PP-PEMs exhibited excellent chemical

stability because of the lack of vulnerable heteroatom bonds in the main chain (e.g., ether, sulfone, and ketone groups which were included in most aromatic polymer-based PEMs). Furthermore, PP-PEMs were highly proton conductive, even at high temperature, when having high density of sulfonic acid groups (or high ion exchange capacity; IEC). Some PP-PEMs were claimed to exhibit comparable fuel cell performance with the benchmark Nafion membrane.^{20–23} For example, sulfonated, phenylated PP-PEMs (SPPB- H^+ membranes) developed by Holdcroft et al. exhibited greater peak power density (1237 mW cm^{-2} supplying H_2/O_2 and 587 mW cm^{-2} supplying H_2/air) than that of Nafion NRE 212 membrane (793 mW cm^{-2} supplying H_2/O_2 and 455 mW cm^{-2} supplying H_2/air) and 4-fold longer lifetime than that of Nafion NRE 211 membrane (withstanding 400 h in OCV hold test for SPPB- H^+ but only 100 h for Nafion NRE 211 until the OCV decreased below 0.7 V) at 90 °C, 30% RH and H_2/air .²¹ We have developed several kinds of PP-PEMs with simpler chemical structure. Among them, SPP-QP-f having tetrafluorophenylene groups in the hydrophobic component exhibited high proton conductivity and comparable fuel cell performance with Nafion NRE 211 membrane because the partial fluorinated structure contributed to the interfacial compatibility with the Nafion-based catalyst layers. The average decay of OCV was as low as $118\text{ }\mu\text{V h}^{-1}$ for 1000 h proving the excellent chemical durability of SPP-QP-f.²³ Besides, in the practical fuel cell operation, mechanical durability is another crucial factor directly affecting the lifetime of the cells while few reports focused on this issue.^{24–26} PP-PEMs carrying high IECs absorb more water than that of Nafion, exhibit smaller tensile properties and thus, often encounter mechanical failure based on large swelling/ shrinking in the operating fuel cells.

^a Graduate School of Medical, Industrial and Agricultural Science, University of Yamanashi, Kofu, Yamanashi 400-8510, Japan.

^b Clean Energy Research Center, University of Yamanashi, Kofu, Yamanashi 400-8510, Japan.

^c Fuel Cell Nanomaterials Center, University of Yamanashi, Kofu, Yamanashi 400-8510, Japan.

^d Department of Applied Chemistry, and Research Institute for Science and Engineering, Waseda University, Tokyo 169-8555, Japan.

† Electronic Supplementary Information (ESI) available: See DOI: 10.1039/x0xx00000x

US-DOE proposed a protocol for evaluating the practical lifetime of PEMs by combination of chemical (OCV hold) and mechanical (relative humidity (wet/dry) cycling; RHC) as an accelerated durability test. Mukundan et al.²⁶ reported durability of several PFSA-PEMs in the combined chemical and mechanical durability test (OCV/RHC). Ballard HD6 and P5 membranes showed significant increase in the gas permeability after 1500 and 3000 cycles, respectively, due to the chemical degradation. Even the reinforced PFSA-PEM, Nafion-XL reinforced with a thin porous expanded PTFE (ePTFE) substrate, failed after ca. 9000 cycles. We have recently reported that ePTFE-reinforced, partially fluorinated PP-PEMs exhibited durability in the OCV/RHC test up to 2300 cycles with no obvious structural changes detected in the NMR spectra of the post-test membrane.²⁷

There have been no aromatic polymer-based, non-reinforced PEMs that successfully survived more than several thousand cycles in the combined chemical and mechanical (OCV/RHC) durability test. The objective of the present research is to achieve comparable or even higher performances (*e.g.*, fuel cell performance and combined chemical and mechanical durability) than those of the PFSA-PEMs under severe conditions through tuning the main chain structure and substituent groups of PP-PEMs (without additives and/or physical reinforcement).

Experiments

Materials. 1,4-Bis(trifluoromethyl)benzene (Apollo Scientific), N-bromosuccinimide (NBS, TCI), 3-chlorophenylboronic acid (TCI), 2,5-dichlorobenzenesulfonic acid dehydrate (SP, TCI), bis(1,5-cyclooctadiene)nickel(0) (Ni(COD)₂ TCI), 2,2'-bipyridine (BPY, TCI), and other chemicals and solvents were purchased and used as received.

Synthesis of 2,5-dibromo-3,6-bis(trifluoromethyl)benzene (BFB). A 100-mL flask was filled with 1,4-bis(trifluoromethyl)benzene (1.50 g, 7 mmol), trifluoroacetic acid (20 mL) and concentrated sulfuric acid (5 mL) and heated at 70 °C in an oil bath for 30 min. After cooling to 60 °C, NBS (3.74 g, 21 mmol) was added to the mixture. After the reaction for 48 h, the mixture was poured into large excess of water to precipitate the product. The crude product was washed with water several times, recrystallized from ethanol to obtain 2,5-dibromo-3,6-bis(trifluoromethyl)benzene (BFB) in 43% yield (1.1 g).

Synthesis of 3,3'-dichloro-2',5'-bis(trifluoromethyl)-1,1':4',1''-terphenyl (TFP). BFB (2.23 g, 6 mmol), 3-chlorophenylboronic acid (2.81 g, 18 mmol), potassium carbonate (1.66 g, 12 mmol), toluene (77 mL), ethanol (45 mL), and water (22 mL) were placed into a 500-mL flask equipped with a reflux condenser. To the mixture, Pd(PPh₃)₄ (0.83 g, 0.72 mmol) was added. The mixture was heated at 70 °C in nitrogen for 18 h. The mixture was then diluted with toluene and washed with brine several times. The organic layer was evaporated to obtain the crude product, which was purified by silica gel column

chromatography (eluent: hexane: dichloromethane= 7: 3). Recrystallization from hexane: dichloromethane= 4: 1 gave 3,3'-dichloro-2',5'-bis(trifluoromethyl)-1,1':4',1''-terphenyl (TFP) in 42% yield (1.09 g).

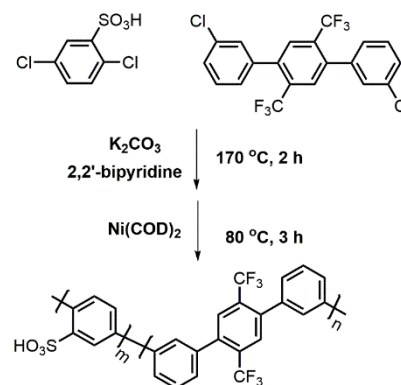
Synthesis of polymers (SPP-TFP). A typical polymerization procedure was as follows. Take SPP-TFP-4.0 (4.0, the feeding IEC) for instance, A three-neck 100-mL flask was charged with TFP (0.31 g, 0.71 mmol), SP (0.73 g, 2.76 mmol), potassium carbonate (0.46 g, 3.31 mmol), BPY (3.27 g, 20.82 mmol), dehydrated toluene (10.5 mL), and dehydrated DMSO (10.5 mL). The mixture was heated at 170 °C for 2 h for azeotropic removal of water. After cooled to 80 °C, Ni(COD)₂ (2.86 g, 10.41 mmol) was added to the mixture. The polymerization reaction was carried out at 80 °C for 3 h. The mixture was poured into 6 M hydrochloric acid to precipitate the product. The crude product was washed with cold 6 M hydrochloric acid and water and dried in vacuum at 70 °C to obtain SPP-TFP-4.0 polymer in 90% yield. SPP-TFPs with other compositions were synthesized in a similar manner.

Preparation of membranes. SPP-TFP solution in DMSO (5wt%) was filtered and cast onto a flat glass plate at 60 °C overnight. The resulting transparent, flexible membrane was washed with 1 M sulfuric acid and water successively.

Results and discussions

Polymer synthesis

The sulfonated polyphenylene (SPP-TFP) consisting of sulfonated phenylene (SP) and bis(trifluoromethyl)-terphenylene (TFP) was synthesized as shown in Scheme 1.



Scheme 1. The synthesis route of SPP-TFP copolymer.

The hydrophobic monomer (TFP) was obtained by bromination of 1,4-bis(trifluoromethyl)benzene and Suzuki-Miyaura coupling reaction successively, as shown in Scheme S1. ¹H and ¹⁹F NMR spectra confirmed the chemical structures of the BFB and TFP, where the peaks were well-assigned to the supposed structures (Fig. S1 and S2). By controlling the feed ratio of SP and TFP, the copolymers (SPP-TFP) with different target ion exchange capacity (IEC=3.0, 3.5, 4.0 mmol g⁻¹) were synthesized via Ni(0)-mediated coupling reaction (Scheme 1). We designed

Table 1. Composition, molecular weight, IEC, yield and swelling ratio of SPP-TFP membranes.

Membrane	Composition		IEC (mmol g ⁻¹)			Molecular weight (kDa)			Yield (%)	Swelling ratio (%)	
	m: n ^a	m: n ^b	Target	NMR	Titred	Mn	Mw	PDI ^c		In-plane	Through-plane
SPP-TFP-3.0	1: 0.48	1: 0.54	3.0	2.83±0.07	2.58±0.06	51.2	196.1	3.8	97	16±2	16±4
SPP-TFP-3.5	1: 0.35	1: 0.42	3.5	3.23±0.08	2.99±0.04	123.4	527.4	4.3	90	19±2	23±7
SPP-TFP-4.0	1: 0.25	1: 0.37	4.0	3.44±0.06	3.40±0.08	104	556.1	5.4	90	20±3	47±8
Nafion NRE211	--	--	--	--	0.97±0.06	--	--	--	--	8.5±0.5	12±6

^a Feed composition; ^b Calculated from the ¹H NMR spectra; ^c Polydispersity index (Mw/Mn). ^d Measured at r.t. under full hydrated state.

to have total *meta/para* phenylene group ratio to be 0.65- 0.4 for improving membrane properties, in particular, mechanical strength and durability. The prepared copolymers were soluble in lower alcohols such as ethanol, as well as in high-boiling polar aprotic solvents (DMSO, DMF et.al.). The solubility was similar to our previously reported poly(*para*-phenylene)s having the same CF₃ substituents (SPP-BP-CF₃).²⁸ The chemical structure of SPP-TFP was analyzed via NMR spectra (Fig. 1a and b). The copolymer composition was estimated from the integral of the proton peaks and summarized in Table 1. The chemical structure of SPP-TFP was further analyzed by FT-IR spectrum. The absorption peaks of stretching vibrations of C=C bonds in phenylene groups appeared at 1407, 1439, 1465, and 1606 cm⁻¹. The absorption peaks at 1138 and 1163 cm⁻¹ were assigned to stretching vibrations of O=S=O bonds of the sulfonic acid groups. The absorption peaks at 1236 and 1301 cm⁻¹ were ascribed to C-F stretching bonds.²⁹ GPC analyses indicated that SPP-TFP copolymers possessed appreciably high molecular weights from 196.1 to 556.1 kDa for M_w and from 51.2 to 123.4 kDa for M_n, respectively, because of the high reactivity of TFP monomer with *meta*-phenylene structure and the electron-drawing CF₃ groups. In fact, the molecular weight of SPP-TFP was much higher than that (M_w = 161-316 kDa, M_n = 49-149 kDa) of SPP-BP-CF₃. Casting the DMSO solution provided bendable transparent membranes from the three copolymers. The titrated IECs were comparable to or only slightly smaller than those calculated from the copolymer compositions. Compared to SPP-BP-CF₃ membranes, SPP-TFP exhibited superior membrane forming capability because of the higher molecular weight and bent *meta*-phenylene groups (or lower persistence length¹⁶) both of which favored random-coil structure resulting in higher mechanical strength.

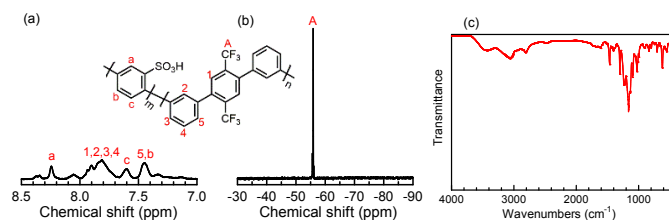


Fig. 1 (a) ¹H and (b) ¹⁹F NMR spectra of SPP-TFP-4.0 in DMSO-*d*₆ at 80 °C. (c) FT-IR spectrum of SPP-TFP-4.0 membrane.

Morphology

The phase-separated morphology of the membranes based on the hydrophilic and hydrophobic differences in the components was characterized by TEM image as shown in Fig. 2, where the hydrophilic (dark) and hydrophobic (bright) domains were composed of aggregated sulfonic acid groups and aromatic groups, respectively. The phase-separation of the membranes developed with more distinct interfaces as increasing the IEC. The hydrophilic domain size was small, 1.7 ± 0.2 nm for SPP-TFP-3.0, 2.2 ± 0.3 nm for SPP-TFP-3.5, and 2.5 ± 0.3 nm for SPP-TFP-4.0, respectively, averaged from more than 100 spots. In contrary, the hydrophobic domain became slightly smaller as increasing the IEC, 2.1 ± 0.3 nm, 1.8 ± 0.2 nm and 1.7 ± 0.2 nm for SPP-TFP-3.0, -3.5 and -4.0, respectively, due to the decreased content of the hydrophobic component. The hydrophilic domain size of SPP-TFP membranes was smaller than that (4.2- 4.4 nm) of our previously reported sulfonated poly(*para*-phenylene) membranes with CF₃ substituents (SPP-BP-CF₃). Since SPP-TFP contained *meta*-phenylene groups (*m*: *p* = 2: 1) in the hydrophobic components, the polymer main chains were likely to have more compact (random-coil like) configurations than SPP-BP-CF₃ which contained only *para*-phenylene groups, resulting in the smaller domain sizes. Similar tendency was observed in the other types of polyphenylene ionomer membranes containing perfluoroalkylene groups;³⁰ *para*-linked SPAF-*p*P-2.66 showed similar hydrophilic domain size (2.5 nm) with *meta*-linked SPAF-*m*P-2.77 (2.5 nm) while the latter contained higher IEC (2.77 mmol g⁻¹).

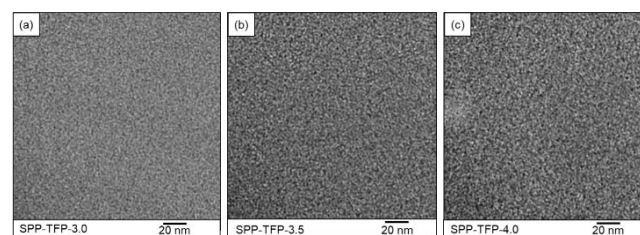


Fig. 2 TEM images of SPP-TFP membranes stained with Pb²⁺ ions under IEC = (a) 3.0, (b) 3.5 and (c) 4.0 mmol g⁻¹.

The small-angle-X-ray scattering (SAXS) patterns of the membranes were obtained at 80 °C and various relative humidity (from 90% to 30% RH). Scattering intensity is plotted as a function of the scattering vector (*q*) in Fig. S3. No obvious peaks were found for those three SPP-TFP membranes at any humidity suggesting that no periodic structure was involved. In fact, the scattering intensity became smaller as increasing the

humidity for SPP-TFP-3.0, -3.5, and -4.0 membranes. The hydrophilic/hydrophobic domains confirmed in the TEM images did not develop homogeneously with the water absorption, but became rather randomized. Similar phenomena were confirmed previously with other types of aromatic ionomer membranes.^{20,28,31}

Water uptake and proton conductivity

Humidity dependence of water uptake of SPP-TFP, SPP-BP-CF₃-3.5, and Nafion NRE 212 membranes was measured at 80 °C (Fig. 3a). As expected, the water uptake increased as increasing humidity. Compared to SPP-BP-CF₃-3.5 membrane, SPP-TFP-3.5 membrane with comparable IEC showed higher water uptake, particularly, at high humidity, probably because *meta*-phenylene groups in the SPP-TFP produced more free volume to absorb more water. The number of absorbed water molecules per sulfonic acid group (λ) was plotted as a function of relative humidity in Fig. S4. While the differences in λ values of SPP-TFP and SPP-BP-CF₃-3.5 membranes were rather minor, their λ values were higher than that of Nafion NRE 212 at high humidity ($\geq 60\%$ RH). Compared with the perfluorinated Nafion membrane in which the hydrophobic domains usually do not contribute to water absorption, hydrophilic/hydrophobic differences were less pronounced for SPP-TFP and SPP-BP-CF₃-3.5 membranes responsible for higher water absorbing capability. Due to the higher water uptake and IEC, the swelling of SPP-TFP-4.0 was 20% (in-plane) and 47% (through-plane) at r.t. under full hydrated state which were higher than those of SPP-TFP-3.0 and -3.5 as listed in Table 1. The anisotropic swelling behavior may be indicative of the aromatic polymer alignment to the horizontal direction.

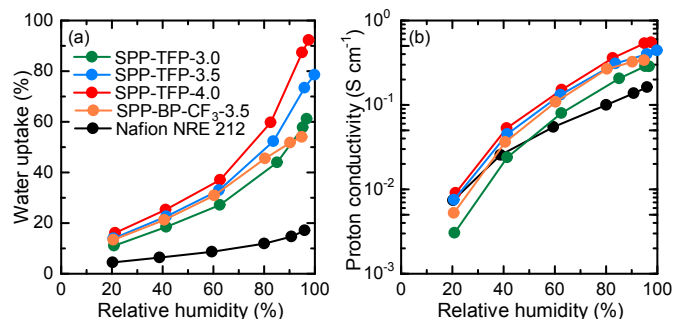


Fig. 3 (a) Water uptake and (b) proton conductivity of SPP-TFP, SPP-BP-CF₃-3.5 and Nafion NRE 212 membranes as a function of relative humidity at 80 °C.

Fig. 3b shows humidity dependence of the proton conductivity of SPP-TFP, SPP-BP-CF₃-3.5 and Nafion NRE 212 membranes measured under the same conditions as water uptake. The proton conductivity of SPP-TFP membranes also increased with the humidity and IEC. The highest IEC SPP-TFP-4.0 membrane exhibited the highest conductivity at any humidity (e.g., 550 mS cm⁻¹ at 95% RH). Then, proton diffusion coefficient (D_0) was calculated from Nernst-Einstein equation and was plotted as a function of volumetric IEC (IEC_v, which took absorbed water into account) in Fig. 4. Compared to Nafion NRE 212 which exhibited significant dependence of the diffusion coefficient on the IEC_v, SPP-TFP and SPP-BP-CF₃-3.5 membranes required higher IEC_v values to achieve the comparable diffusion

coefficient due to the less acidic nature of the aromatic sulfonic acid groups than the perfluoroalkylsulfonic acid groups. Differences in SPP-BP-CF₃-3.5 and SPP-TFP-3.5 membranes would be probably based on the differences in the hydrophilic domain size (4.4 ± 0.2 nm for SPP-BP-CF₃-3.5 and 2.2 ± 0.3 nm for SPP-TFP-3.5) and the absorbed water content, where larger domain size and appropriate water content were both crucial for the proton conduction.

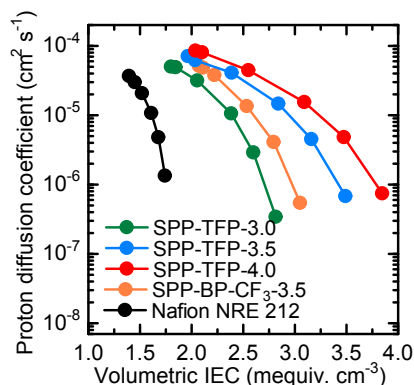


Fig. 4 Proton diffusion coefficient as a function of volumetric IEC (IEC_v of SPP-TFP, SPP-BP-CF₃-3.5 and Nafion NRE 212 membranes at 80 °C.

Mechanical properties

The mechanical properties of SPP-TFP membranes were investigated via tensile tests and dynamic mechanical analyses (DMA). Viscoelastic properties of the SPP-TFP membranes were measured as a function of the relative humidity (at 80 °C) and temperature (at 60% RH) as shown in Fig. S5. The storage modulus (E') and loss modulus (E'') of SPP-TFP decreased as increasing the humidity and the decrease became larger as increasing the IEC because the absorbed water functioned as plasticizer.³³ No glass transition behavior was confirmed under the test conditions proving that the SPP-TFP membranes were thermally stable under a variety of humidity conditions. SPP-TFP membranes retained good thermal stability up to 95 °C, 60% RH, where slight changes were detected in E' , E'' , and $\tan \delta$ curves.

The stress/strain curves were measured at 80 °C and 60% RH as shown in Fig. 5. Compared to our previous polyphenylene-based ionomer SPP-BP-CF₃ membranes, SPP-TFP membranes exhibited excellent tensile properties with the maximum strength (28.1 ± 1.2 - 33.6 ± 0.8 MPa) and maximum strain (84 ± 2 - $155 \pm 5\%$). In particular, higher IEC SPP-TFP-3.5 and -4.0 membranes were much more mechanically robust suggesting that *meta*-phenylene groups (67 mol% in the total phenylene groups in the hydrophobic component) in the main chain and high molecular weight significantly improved the tensile properties. In fact, the tensile properties of unreinforced SPP-TFP-3.5 (33.6 ± 0.8 MPa, $155 \pm 5\%$) and -4.0 (28.1 ± 1.2 MPa, $141 \pm 8\%$) membranes were similar to SPP-QP membrane reinforced with porous polyethylene substrate, which exhibited 47 MPa of the maximum stress and 134% of the maximum strain under the same temperature/humidity conditions.³²

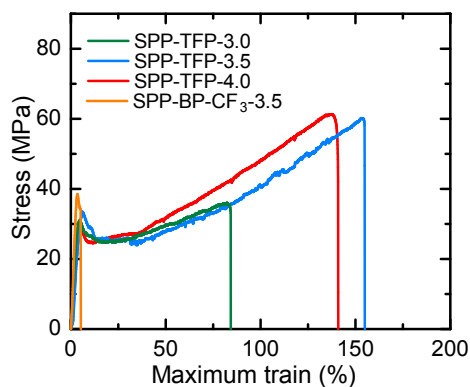


Fig. 5 Stress versus strain curves of SPP-TFP and SPP-BP-CF₃-3.5 membranes at 80 °C under 60% RH.

Thermal stability

Thermal stability of SPP-TFP membranes were investigated via TG analyses. The TG curves are displayed in Fig. S6. The initial weight loss from r.t. to ca. 130 °C was attributable to the evaporation of absorbed water, and in the order, SPP-TFP-4.0 > SPP-TFP-3.5 > SPP-TFP-3.0 since higher IEC membranes absorbed more water. The second weight loss from 250 to 400 °C was associated with the decomposition of the sulfonic acid groups, and was also in the same order. The following third stage above ca. 510 °C resulted from the decomposition of the polymer backbone.

Ex-situ oxidative stability

The *ex-situ* chemical stability of SPP-TFP membranes was scrutinized by subjecting membranes to Fenton's reagent at 80 °C. After 1 h, all membranes remained flexible with minor weight losses (< 5%) as shown in Table S2, suggesting good chemical stability. Further details of the post-test membranes including molecular weight, IEC, and chemical structure were characterized by GPC, acid base titration and NMR spectra. While the loss of IEC was rather minor similar to the weight, that of molecular weight (M_w) was more serious with 63%- 78% remaining. ¹⁹F NMR spectra indicated that the fluorine (trifluoromethyl) groups were intact (Fig. S7). In contrast, the proton peaks 'a and c' in the sulfonated phenylene groups and '2-4' in the phenylene groups of the hydrophobic components declined in the intensity. From those results, we concluded that hydroxy (HO·) groups attacked the sulfonated and neighboring phenylene groups causing losses in the sulfonic acid groups, and accordingly losses in weight, IEC and molecular weight. Nevertheless, since the oxidative degradation was rather minor, the post-test membranes retained the water affinity and proton conductivity at a wide range of the humidity (Fig. S8). As shown in Fig. S9, the post-test membranes retained viscoelastic properties with negligible changes. Overall, SPP-TFP membranes exhibited excellent oxidative stability in Fenton's test because of chemically robust polyphenylene main chain structure.

Fuel cell performance

Because of excellent mechanical properties and high proton conductivity under high and low humidity conditions, SPP-TFP-3.5 (31 μm thick) and -4.0 (28 μm thick) were selected to fabricate the membrane electrode assemblies (MEA) for fuel cell evaluation. Prior to IV (polarization) measurement, linear sweep voltammogram (LSV) was taken to estimate the hydrogen permeability of the membranes at 80 °C at 100% and 30% RH supplying H₂ and N₂ to the anode and the cathode, respectively. As shown in Fig. S10, at 100% RH, the hydrogen crossover current density of SPP-TFP-3.5 (0.282 mA cm⁻²) and SPP-TFP-4.0 (0.884 mA cm⁻²) was lower than that of Nafion NRE 211 (1.27 mA cm⁻²), suggesting the lower H₂ permeability of the SPP-TFP membranes. Higher H₂ permeability of SPP-TFP-4.0 than that of SPP-TFP-3.5 was the result of higher swellability of the higher IEC membrane. At 30% RH, the H₂ crossover current density slightly decreased compared to 100% RH, in particular, at high potential supporting this idea.

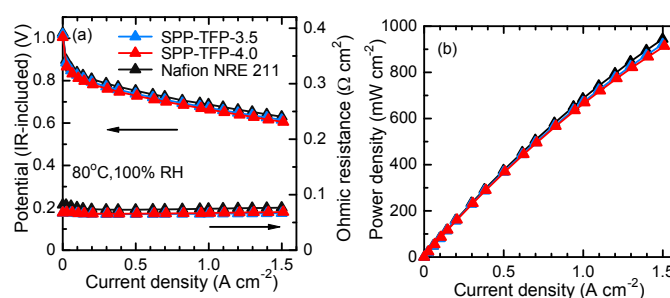


Fig. 6 (a) IR-included polarization curves and ohmic resistances as well as (b) power density of SPP-TFP-3.5 (31 μm), -4.0 (28 μm) and Nafion NRE 211 (25 μm) cells under H₂/O₂ at 80 °C and 100% RH.

The polarization curves were measured at 80 °C under 100% and 30% RH supplying O₂ to the cathode and H₂ to the anode without backpressure. Profiting from the low hydrogen permeability, SPP-TFP-3.5 and -4.0 cells exhibited high open circuit voltage (OCV) (> 0.97 V) at both humidities. At 100% RH (Fig. 6a), the SPP-TFP-3.5 and -4.0 cells showed the same ohmic resistance (0.067 Ω cm²), which was higher than that calculated from the thickness and proton conductivity (0.007 Ω cm² for SPP-TFP-3.5 and 0.005 Ω cm² for SPP-TFP-4.0) due to the contact resistance between the catalyst layers and membrane. The IV performance of those cells was comparable to that of Nafion membranes up to 1.5 A cm⁻² of the current density. At 1.5 A cm⁻² (Fig. 6b), the maximum power density reached 921.8 mW cm⁻², 913.7 mW cm⁻² and 944.2 mW cm⁻² for SPP-TFP-3.5, -4.0 and Nafion NRE 211 cells, respectively. At 30% RH (Fig. S11a), the ohmic resistance of SPP-TFP-4.0 (0.264 Ω cm²) was lower than that of SPP-TFP-3.5 (0.368 Ω cm²) reflecting its higher proton conductivity. The ohmic resistance decreased to 0.149 Ω cm² for SPP-TFP-3.5 and to 0.115 Ω cm² for SPP-TFP-4.0 with increasing the current density owing to the back-diffusion of the product water from the cathode into the membranes. Although the ohmic resistance was comparable, SPP-TFP-3.5 and -4.0 cells were slightly inferior in the IV performance, in particular, at higher current density to Nafion cell, probably due to the minor incompatibility with the catalyst layers. At 1.5 A cm⁻² (Fig. S11b), the maximum power density was 647.5 W cm⁻².

² for SPP-TFP-3.5 cell, 706.8 W cm⁻² for SPP-TFP-4.0 cell and 785.4 W cm⁻² for Nafion cell.

Combined chemical and mechanical durability

As reported in the literature, sulfonated polyphenylene type proton exchange membranes (SPP-PEMs) without any heteroatom groups in the main chain exhibited oxidative stability as evidenced in 1000-h OCV hold test durability.¹⁶ However, because of large water absorbability (ca. 40 wt% at 90% RH) and relatively small strain (< 100% of the maximum strain in stress/strain curves), those SPP-PEMs were not mechanically robust and thus, to successfully survive the wet/dry cycling test, soft gas diffusion layer (GDL)³⁴ or physical reinforcement³¹ was required at some expense of fuel cell performance.

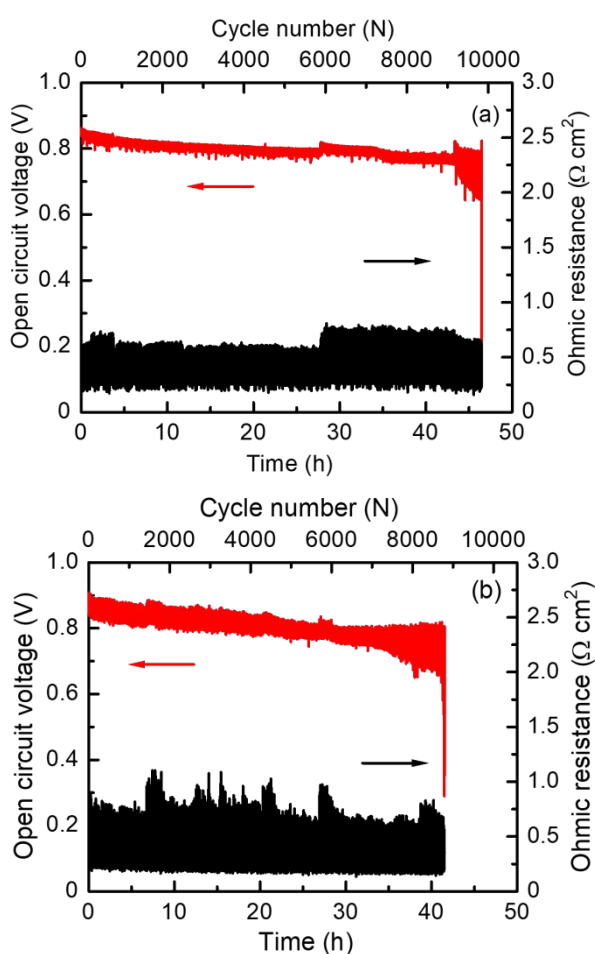


Fig. 7 The OCV and ohmic resistance of (a) SPP-TFP-3.5 and (b) Nafion NRE 211 during the combined chemical and mechanical durability test at 90 °C with frequent wet and dry cycling supplying H₂ (0.06 L min⁻¹, anode) and air (0.06 L min⁻¹, cathode).

In the present study, considering excellent mechanical properties and low swelling ratio, SPP-TFP-3.5 membrane was chosen for the combined chemical and mechanical durability (OCV/RHC) test. The test conditions included frequent humidity cycling under OCV conditions, where the intervals of wet and dry gases were determined to be 2 and 15 s, respectively, to

ensure the difference in the ohmic resistance larger than 2.5 times. The OCV was initially 0.862 (100% RH) and 0.847 V (0% RH), and decreased gradually with the testing time (Fig. 7). After 9847 cycles (or 46.5 h), the OCV showed a sudden drop, suggesting mechanical failure of the membrane. The average decay of the OCV during the test was as low as 2 mV h⁻¹. It should be noted that SPP-TFP-3.5 membrane with no physical reinforcement survived much more than our partially fluorinated SPP-PEMs reinforced with porous ePTFE (SPP-TP-f-5.1/DPTFE) (2300 cycles) under the same conditions.²⁷ In contrast, Nafion NRE 211 membrane only survived 8788 cycles (or 41.5 h) with 3 mV h⁻¹ of the average OCV decay. To the best of our knowledge, SPP-TFP-3.5 membrane is the first and only aromatic polymer-based, unreinforced PEM that outperformed Nafion membrane in the combined chemical and mechanical durability test.

After the test, the cell was disassembled and the recovered membranes kept flexibility without obvious cracks but several pinholes (Fig S12) causing the sudden drop in the OCV to terminate the test. The post-test membrane was subjected to NMR and GPC analyses (Fig. S13 and Table S3). While the ¹⁹F NMR spectrum did not change, the ¹H NMR spectra showed minor changes in some aromatic protons accounting for 7.5% loss of the sulfonic acid groups estimated from the peak integrals. The molecular weight decreased to ca. 70% that of the pristine membrane due to the loss of the sulfonic acid groups and the following minor main chain degradation. The decrease in the molecular weight affected much on the mechanical properties as evidenced in the stress/ strain curve (Fig. S14), where the maximum strain of the post-test membrane was 23% compared to 155% of the pristine membrane. Mechanical properties of Nafion NRE 211 membrane were also deteriorated, with 26% of the maximum strain for the post-test compared to 391% of the pristine membrane.

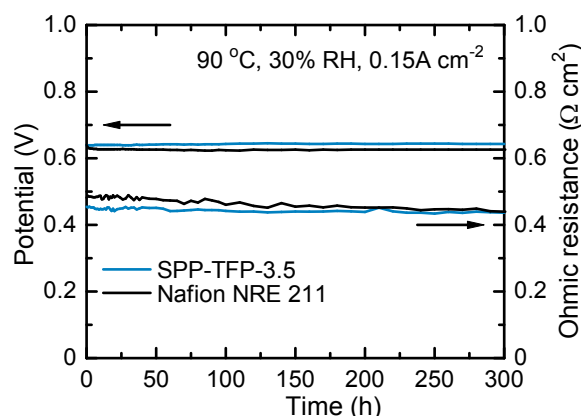


Fig. 8 The durability test of SPP-TFP-3.5 and Nafion NRE 211 membranes at a constant current density (0.15A cm⁻²) under 90 °C and 30% RH, supplying hydrogen (0.1 L min⁻¹) and air (0.1 L min⁻¹) at anode and cathode, respectively.

The durability test of SPP-TFP-3.5 and Nafion NRE 211 membranes were further carried out at a constant current density (0.15 A cm⁻²) under 90 °C and 30% RH as shown in Fig. 8. After 300 h, the cell voltage exhibited negligible change from 0.639 to 0.643 V for SPP-TFP-3.5 while the cell voltage declined from 0.640 V to 0.626 V at 46.7 μV h⁻¹ of the average decay for

Nafion NRE 211. The results also suggest that the SPP-TFP-3.5 membrane was more durable than Nafion NRE 211 membrane in operating fuel cells.

Conclusions

Novel sulfonated polyphenylene ionomers, SPP-TFP, were synthesized by the Ni(0)-promoted polycondensation of commercial sulfonated dichlorobenzene (SP) and newly prepared dichloro-bis(trifluoromethyl)terphenyl (TFP) monomers. By controlling the feed ratio of TFP and SP comonomers, the resulting copolymers contained different concentration of the sulfonic acid groups (IEC = 3.0- 4.0 mmol g⁻¹) and high molecular weight (M_n = 51.2- 123.4 kDa and M_w = 96.1- 556.1 kDa). Despite the rigid polyphenylene main chain structure, the combination of *meta*-phenylene groups and trifluoromethyl substituents contributed to providing the copolymers with good membrane forming capability. In fact, the resulting SPP-TFP membranes exhibited slightly higher proton conductivity (7.5 mS cm⁻¹ at 20% RH) and much better mechanical properties (155 ± 5% of the maximum strain) compared to those (5.2 mS cm⁻¹ at 20% RH and 5.2 ± 0.8% of the maximum strain) of our previous sulfonated, trifluoromethylated poly(*para*-phenylene) SPP-BP-CF₃ membranes with comparable IEC. The selected SPP-TFP-3.5 membrane displayed comparable fuel cell performance (921.8 mW cm⁻² for the maximum power density at 1.5 A cm⁻² at 100% RH) and lower gas permeability (0.282 mA cm⁻² at 100% RH) compared to state-of-the art Nafion NRE 211 membrane. The durability of SPP-TFP-3.5 membrane was assessed via the accelerated, combined chemical (OCV hold) and mechanical (wet/dry cycling) test at 90 °C according to the US-DOE protocol. The membrane survived (9847 cycles), surpassing Nafion NRE 211 membrane (8788 cycles). To the best of our knowledge, this is the first example that the aromatic polymer-based proton conductive membrane without any chemical/physical reinforcement exhibited such outstanding durability. The post-test membrane, however, showed slight changes in the chemical structure and some loss in mechanical properties, which were the indications of the main chain scission possibly triggered by the degradation of the sulfonic acid groups. Further improvement in the durability of sulfonated polyphenylene membranes is in our future agenda.

Conflicts of interest

There are no conflicts to declare.

Author contributions

Fanghua Liu: Methodology, investigation, and writing
Kenji Miyatake: Supervision, conceptualization, writing, reviewing and editing, funding acquisition, and project administration

Acknowledgements

We thank Dr. Akihiro Masuda of Toray Research Center for cross-sectional SEM images. This work was partly supported by the New Energy and Industrial Technology Development Organization (NEDO), the Ministry of Education, Culture, Sports, Science and Technology (MEXT), Japan, through Grants-in-Aid for Scientific Research (18H05515), Japan Science and Technology (JST) through SICORP (JPMJSC18H8), JKA promotion funds from AUTORACE, the thermal and electric energy technology foundation and the China Scholarship Council (CSC).

References

- 1 Y. Wang, D. F. R. Diaz, K. S. Chen, Z. Wang and X. C. Adroher, *Mater. Today*, 2020, **32**, 178-203.
- 2 C. Klose, T. Saatkamp, A. Münchinger, L. Bohn, G. Titvinidze, M. Breitwieser, K. D. Kreuer and S. Vierrath, *Adv. Energy Mater.*, 2020, **10**, 190399-1904003.
- 3 Y. Gao, G. P. Robertson, M. D. Guiver, S. D. Mikhailenko, X. Li and S. Kalishuine, *Macromolecules*, 2005, **38**, 3237-3245.
- 4 R. Borup, J. Meyers, B. Pivovar, Y. S. Kim, R. Mukundan, N. Garland, D. Myers, M. Wilson, F. Garzon, D. Wood, P. Zelenay, K. More, K. Stroh, T. Zawodzinski, J. Boncella, J. E. McGrath, M. Inada, K. Miyatake, M. Hori, K. Ota, Z. Ogumi, S. Miyata, A. Nishikata, Z. Siroma, Y. Uchimoto, K. Yasuda, K. Kimijima and N. Iwashita, *Chem. Rev.*, 2007, **107**, 3904-3951.
- 5 D. E. Curtin, R. D. Lousenberg, T. J. Henry, P. C. Tangeman and M. E. Tisack, *J. Power Sources*, 2004, **131**, 41-48.
- 6 T. Kinumoto, M. Inaba, Y. Nakayama, K. Ogata, R. Umebayashi, A. Tasaka, Y. Iriyama, T. Abe and Z. Ogumi, *J. Power Sources* 2006, **158**, 1222-1228.
- 7 S. Holdcroft, *Chem. Mater.*, 2014, **26**, 381.
- 8 M. P. Rodgers, L. J. Bonville, H. R. Kunz, D. K. Slattery and J. M. Fenton, *Chem. Rev.*, 2012, **112**, 6075-6103.
- 9 M. Adamski, N. Peressin and S. Holdcroft, *Mater. Adv.*, 2021, **2**, 4966-5005.
- 10 T. Holmes, T. J. G. Skalski, M. Adamski and S. Holdcroft, *Chem. Mater.*, 2019, **31**, 1441-1449.
- 11 P. Pei, and H. Chen, *Appl. Energy*, 2014, **125**, 60-75.
- 12 M. Litt, G.-F. Sergio, K. Junwon, S. Kun and R. Wycisk, *RCS Trans.*, 2010, **33**, 695-710.
- 13 K. Si, R. Wycisk, D. Dong, K. Cooper, M. Rodgers, P. Brooker, D. Slattery, and M. Litt, *Macromolecules*, 2013, **46**, 422-433.
- 14 T. J. G. Skalski, B. Britton, T. J. Peckham and S. Holdcroft, *J. Am. Chem. Soc.*, 2015, **137**, 12223-12226.
- 15 H. Nguyen, F. Lombeck, C. Schwarz, P. A. Heizmann, M. Adamski, H. -F. Lee, B. Britton, S. Holdcroft, S. Vierrath and M. Breitwieser, *Sustainable Energy Fuels*, 2021, **5**, 3687-3699.
- 16 J. Miyake, R. Taki, T. Mochizuki, R. Shimizu, R. Akiyama, M. Uchida and K. Miyatake, *Sci. Adv.*, 2017, **3**, eaao0476.
- 17 K. H. Lee, J. Y. Chu, A. R. Kim and D. J. Yoo, *Polymers*, 2018, **10**, 1367-1381.
- 18 K. Kim, P. Heo, W. Hwang, J. -H. Baik, Y. -e. Sung and J. -C. Lee, *ACS Appl. Mater. Interfaces*, 2018, **10**, 21788-21793.
- 19 M. Danilczuk, S. Schlick and F. D. Com, *Macromolecules*, 2013, **46**, 6110-6117.
- 20 J. Ahn, R. Shimizu and K. Miyatake, *J. Mater. Chem. A*, 2018, **6**, 24625-24632.
- 21 M. Adamski, T. Skalski, B. Britton, T. Peckham, L. Metzler and S. Holdcroft, *Angew. Chem.*, 2017, **129**, 9186-9189.
- 22 T. Mochizuki, M. Uchida and K. Miyatake, *ACS Energy Lett.*, 2016, **1**, 348-352.
- 23 Z. Long and K. Miyatake, *ACS Appl. Mater. Interfaces*, 2021, **13**, 15366-15372.

ARTICLE

Journal Name

- 24 Y. P. Patil, W. L. Jarrett and K. A. Mauritz, *J. Membr. Sci.*, 2010, **356**, 7-13.
- 25 C. Lim, L. Ghassemzadeh, F. V. Hove, M. Lauritzen, J. Kolodziej, G. Wang, S. Holdcroft and E. Kjeang, *J. Power Sources*, 2014, **257**, 102-110.
- 26 R. Mukundan, A. M. Baker, A. Kusoglu, P. Beattie, S. Knights, A. Z. Weber and R. L. Borup, *J. Electrochem. Soc.*, 2018, **165**, F3085-F3093.
- 27 Z. Long and K. Miyatake, *iScience*, 2021, **24**, 102962-102976.
- 28 F. H. Liu, J. Ahn, J. Miyake and K. Miyatake, *Polym. Chem.*, 2021, **12**, 6101-6109.
- 29 R. Mukherjee, A. K. Mandal and B. Susanta. *e-Polymers*, 2020, **20**, 430-442.
- 30 Z. Long, J. Miyake and K. Miyake, *Bull. Chem. Soc. Jpn.*, 2020, **93**, 338-344.
- 31 K. Shiino, T. Otamo, T. Yamada, H. Arima, K. Hiroi, S. Takata, J. Miyake and K. Miyatake, *ACS Appl. Polym. Mater.*, 2020, **2**, 5558-5565.
- 32 J. Miyake, T. Watanabe, H. Shintani, Y. Sugawara, M. Uchida and K. Miyatake, *ACS Mater. Au*, 2021, **1**, 81-88.
- 33 Y. Zhang, J. Miyake, R. Akiyama, R. Shimizu and K. Miyatake, *ACS Appl. Energy Mater.*, 2018, **1**, 1008-1015.
- 34 T. Tanaka, H. Shintani, Y. Sugawara, A. Masuda, N. Sato, M. Uchida and K. Miyatake, *J. Power Sources*, 2021, **10**, 100063-100068.